# CALCULUS OF OPTICAL LOSSES IN HELIOSTATS FOR CSP WITH LINEAR FRESNEL TECHNOLOGY

**Caio Barreto Vianna Martins, caiobarretovm@hotmail.com**
**Gabriel Ivan Medina Tapia, gmedinat@ct.ufrn.br**
Mechanical Engineering Departament, Universidade Federal do Rio Grande do Norte, Campus Universitário, 3000, Lagoa Nova, Natal, 59072-970, Brazil

***Abstract.*** *In this work a study was elaborated to quantify the optical losses that exist in the tracking and energy concentration system from a CSP plant that uses linear Fresnel reflecting mirrors. The calculated losses were: blocking loss, shading loss, shading loss caused by the receiver, loss by cosine effect, spillage loss, loss due to material reflectivity, tracking system loss and loss due to maintenance. From the loss calculations made, a model was developed to analyze the efficiency of the reflectors of the system over a day, based on the optical performance calculated from the reflected Direct Normal Irradiance (DNI) onto the absorber. Additionally, a sensitivity analysis was performed to assess the influence of some system variables in the energy concentration and thereby choose the geometric parameters of the LRF system so that it produces as much power as possible. Thus, the optimized system was used to generate the simulation of the optical performance of the reflective mirrors in the city of Natal, Rio Grande do Norte. From the results, it is concluded that the developed model generates data close to reality and shows the great solar potential in Northeast region, based on climatic data from the analyzed city.*

***Keywords****: Optical Losses, Heliostats, LFR, CSP.*

## 1. INTRODUCTION

The increasing energy demand in the world, the depletion of traditional energy sources and the environmental impact caused by them has motivated the development and exploration of new technologies for the power generation. Inside this context, there is the possibility of the renewable energy sources exploration. In addition to being considered inexhaustible sources of energy, their exploitation causes less environmental damage than the generation of energy from fossil fuels.

A sustainable energy source that has been better utilized in recent years in the world is solar energy. The sun provides the Earth each year a lot of energy, approximately 1.5 x $10^{18}$ kWh, about 10,000 times the world energy consumption (Eustáquio, 2011). The major limitations of this energy source are the low flux density received on earth (W / m²); intermittence and; the greatest amount of energy available being mainly located in remote areas of the planet (Goswami, 2015).

Brazil is a country with great potential for power generation from solar radiation. It is known that the average annual DNI is above 2000 kWh / m² in many regions of the country (SolarGIS, 2014). It is also known that the Northeast is a region that presents favorable conditions in terms of solar radiation for the production of energy. According to Cordeiro (1998), favorable locations for the installation of solar power plants in Brazil, as previous studies have shown, are the São Francisco River basin and the area of Sobradinho, in the northeastern region.

Despite this great potential, Brazil still has a very concentrated energy matrix in a single source, hydroelectric energy. According to Raia (2016), 64.37% of the energy generated in the country comes from hydroelectric power. Meanwhile, solar energy is underexplored. The water crisis occurred in Brazil in 2015 showed that the concentration of the energy matrix in only one source can compromise the supply of a country's energy demand and consequently impair its operation and development. Thus, alternative energy sources have been studied and explored for the development of new energy collection systems.

One of these new developed systems is the system that uses solar concentrators to convert solar energy into thermal or electrical energy (Concentrated Solar Power - CSP). The CSP systems can make a huge contribution to solve energy problems in a relatively short time, and a great alternative especially for countries with high incidence of solar radiation during the year, which is the case of Brazil. There are four types of CSP technology: parabolic trough, dish Stirling, linear Fresnel reflectors (LFR) and central receiver system (CRS).

Although there CSP technologies with different configurations, all of them have problems which decrease system efficiency. The main loss mechanisms present in these power transformer systems are caused by: cosine effect, shading and blocking by adjacent mirrors, shading by the receiver and spillage.

The loss mechanisms analysis shows clearly that most of them are influenced by the position of the reflecting mirrors relative to the Sun and the receiver. In addition, it is known that the system efficiency depends of local weather conditions. Therefore, in this work, the operation of a CSP system in Natal, Rio Grande do Norte, will be analyzed in order to better understand its operation.

Although there are various CSP technologies, the system that uses linear Fresnel reflectors was chosen due to work simplification and being a promising technology because of the low cost. Linear Fresnel CSP technology is the oldest

technology of the four mentioned above. The first LFR were built in the 1960s, but in the following decades, it lost space for systems with central receptors (Eustáquio, 2011). The LFR systems are composed of several rows of plan reflectors and a suspended linear receiver. The rows of reflectors are placed in parallel and move in a single axis tracking the position of the sun to reflect solar radiation to the linear receiver, which is suspended and fixed above the set of rows. Thus, the fluid passing through the receiver absorber tube is heated and used to generate steam. The steam generated is used to drive a turbine that generates electricity (Baharoon et al., 2014).

For this study will be needed meteorological data of each month of the year from the chosen location and will be developed a model to analyze the system efficiency over a year. In this model will take into account local climatic conditions, the solar position throughout the year and the influence of the loss mechanisms in system efficiency. Finally, the data generated from this analysis will be compared to verify the feasibility of the implementation of this system.

## 2. MATHEMATICAL ANALYSIS OF THE SYSTEM

The aim of the program creation is to model the operation of the primary reflectors from a specific LFR system and simulate its performance. The primary reflectors should move in a way that they reflect the Direct Normal Irradiance (DNI) toward the horizontal receiver located above them with the minimum possible optical loss. To develop this tracking model, it was used as base the models of horizontal absorbers provided by Mathur et al. (1991) and Walker (2013). The model suggested by Walker (2013) suggests that the azimuthal angles and zenith of the sun vector at any time of the day should be designed in the East-West plan for the analysis of the reflection of the mirrors on the receiver, oriented in north-south direction, become two dimensional. Figure 1 below shows the desired two-dimensional projection of the system.

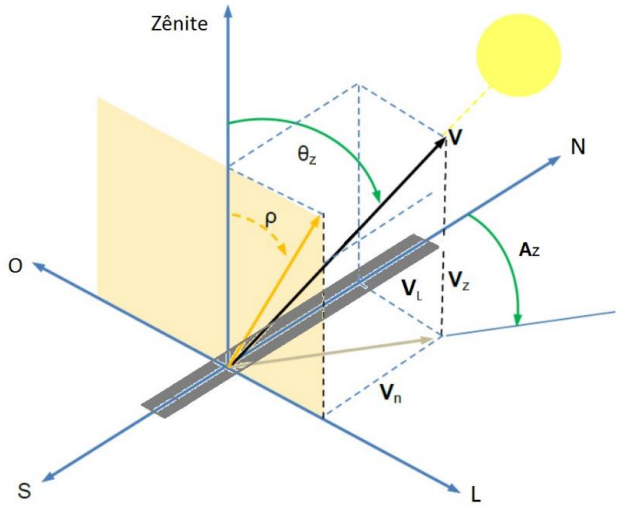


Figure 1. Coordinate system for solar angles (Walker, 2013).

The vector $\boldsymbol{V}$ pointing to the center of the sun can be decomposed into three components in the orthogonal coordinate system shown in Eqs. (1) to (3) below.

$$V_Z = V\cos\theta_Z \tag{1}$$

$$V_n = V\sin\theta_Z\cos A_Z \tag{2}$$

$$V_L = V\sin\theta_Z\sin A_Z \tag{3}$$

Where $\theta_z$ is the zenith angle and $A_z$ is the azimuthal angle. The solar incident angle $\rho$ is calculated by Eq. (3.4).

$$\rho = \arctan\left(\frac{V_n}{V_Z}\right) = \arctan\left(\frac{\sin\theta_Z\sin A_Z}{\cos\theta_Z}\right) \tag{4}$$

For any $n$ reflecting mirror, the incident solar ray in the center of the mirror should, after reflection, reaches the center of the receiver as shown in Fig. 2. For this occur, each mirror n must be inclined by an angle $\theta_n$ from the horizontal plane.

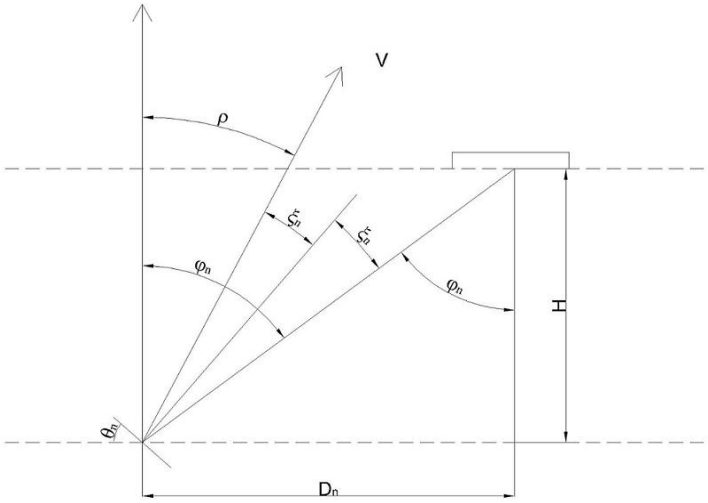


Figure 2. Representation in the coordinate system of the reflection phenomenon and irradiation incidence at the center of the receiver.

From the geometric analysis of the reflection phenomenon and irradiation incidence at the center of the receiver, it is possible to determine the angle of inclination of the mirrors $\theta_n$ in Eq. (6).

$$\theta_n = \frac{\varphi_n + \rho}{2} \tag{6}$$

Where $\xi_n$ is the angle between the incident solar ray in the reflecting mirror and the axis normal to its surface. According to Snell's Law (Tipler, 2012), the angle that determines the direction of the solar ray reflected towards the normal of mirror surface is the same as the angle formed by the incident ray. The angle of incidence on the receiver, $\varphi_n$ is given by Eq. (7).

$$\varphi_n = \arctan\left(\frac{D_n}{H}\right) \tag{7}$$

In this equation, $D_n$ is the horizontal distance between the center of the reflecting mirror n and the receiver center and $H$ is the receiver height in relation to the horizontal axis on which lie the center of rotation of all the reflecting mirrors.

### 2.1 Calculus of losses in the system

There a number of losses occurring in the system. Some of these losses are a result of the geometry design of the system. Others are associated with mechanical losses and material proprieties of the mirrors.

One of the losses occurring in the LFR system is the blocking loss. This loss occurs when part of the rays reflected by a mirror is blocked by adjacent mirror. Figure 3 shows the Sun positioned at a height in the east and a mirror *n* being blocked by a mirror positioned in the next row, mirror *n + 1*.

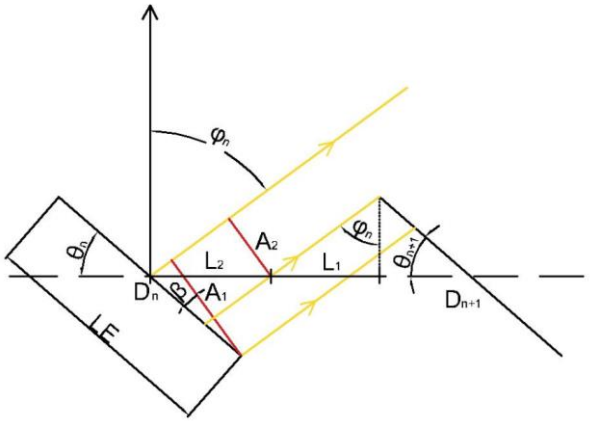


Figure 3. Blocking loss representation.

Where $LE$ is reflecting mirror width, $A_1$ is the half of effective reflection width of the mirror, $A_2$ is the half of effective reflection width of the mirror subtracted the width blocked by adjacent mirror, $L_1$ is the horizontal distance between the edge of the effective width not blocked and the adjacent edge mirror, and $L_2$ is the horizontal distance between the edge of the effective width not blocked and the center of the reflecting mirror $n$. From a geometrical analysis, $A_1$ and $A_2$ are given by Eqs. (8) and (9).

$$A_1 = \frac{LE}{2}\cos(\varphi_n - \theta_n) \tag{8}$$

$$A_2 = \left\{D - \left[\frac{LE}{2}\tan(\varphi_n)\sin(\theta_{n+1})\right] - \left[\frac{LE}{2}\cos(\theta_{n+1})\right]\right\}\sin(90 - \varphi_n) \tag{9}$$

The efficiency related to blocking loss is given by Eq. (10).

$$\eta_{bloc} = \frac{A_1 + A_2}{2A_1} \tag{10}$$

Another loss present in the system is the shading loss. This loss occurs when part of the incident rays in a mirror is blocked by the mirror adjacent. The analysis of this loss is close to the analysis made to blocking loss. Thus, half of effective incidence width of the mirror subtracted from the width shaded by adjacent mirror, $A_4$, is calculated by Eq. (11).

$$A_4 = \left\{D - \left[\frac{LE}{2}\tan(\varphi_n)\sin(\theta_{n+1})\right] - \left[\frac{LE}{2}\cos(\theta_{n+1})\right]\right\}\sin(90 - \rho) \tag{11}$$

Another optical loss that should be considered is the loss by the cosine effect. When the sunray falls in mirror $n$, there is an angle between incident ray and the normal to the mirror n surface as a condition to the reflected beam reaches the receiver. The efficiency equation for this loss is given by Eq. (12).

$$\eta_{\cos} = \frac{A_{refn}}{A_{esp}} = \cos\xi_n \tag{12}$$

Where $A_{ref\,n}$ is the reflected area and $A_{esp}$ is the mirror area.

In addition to shading that a reflector mirror may cause in another mirror, there is also the shading caused by the receiver in the reflective surface. Its efficiency can be calculated by the Eq. (13).

$$\eta_{shad\,\mathrm{Re}\,c} = \frac{A_{incT} - A_{rec}}{A_{incT}} \tag{13}$$

Where $A_{incT}$ is total effective incidence width and $A_{rec}$ is the percentage of receiver width shading the $A_{incT}$.

The spillage is another type of loss that occur in the energy concentration process. This loss occurs when the reflected solar ray does not reach the receiver and is mainly related to flatness of the material surface that reflects the solar rays. In this work was considered that the spillage loss is a function of the distance between the centers of the mirror and the receiver, as shown in Eq. (14).

$$\eta_{spill} = 0.99 - 0.02\sqrt{D_n^2 + H^2} \tag{14}$$

More three losses were considered in this study. The efficiencies related to these losses were obtained from other studies.The reflectivity of the mirror material, $\eta_{ref}$, is equal to 0.94 (Duffie, J.A. and Beckman, W. A., 2013). The efficiency of losses related with the tracking system, $\eta_{track}$, is equal to 0.90 and efficiency of losses related with the maintenance, $\eta_{man}$, is equal to 0.98 for all mirrors. (Sattler et al., 2012).

### 2.2 Calculus of Total Efficiency

From the efficiency of each reflector mirror, it is possible to determine the overall efficiency of the reflector mirror system. The total efficiency of each reflecting mirror can be provided by the product of the unique losses.

$$\eta_{ER,i} = \eta_{bloc}\eta_{shad}\eta_{\cos}\eta_{shad\,\mathrm{Re}c}\eta_{spill}\eta_{ref}\eta_{track}\eta_{man} \tag{15}$$

Where $\eta_{ER,i}$ is the efficiency of each reflecting mirror.
The total efficiency of all reflecting mirrors is given by Eq. (16).

$$\eta_{ER} = \frac{\sum_{i=1}^{N}\eta_{ER,i}A_{ER,i}}{A_{ER}} \tag{16}$$

Where $A_{ER,i}$ is the area of each reflecting mirror (m²) e $A_{ER}$ is the area of all reflecting mirrors (m²).

## 3. RESULTS

Before generating results related to energy directed to the receiver, it is necessary to determine the geometric parameters of the LFR system. During the software creation process, some variables were taken into account, and to understand the influence of some of them in the system's operation, some sensitivity analysis were made.

To facilitate the analysis and understanding of the data generated, it was chosen to maintain a constant DNI equal to 888 W / m² and a Sun period of 13h. Initially, four mirrors widths were considered for analysis. The distance between mirrors is10 cm, the horizontal distance between the center of the receiver and the nearest mirrors is 40 cm, the receiver size should be 10 cm greater than the width of the reflecting mirrors and the length of the mirrors was considered equal to 3 m. The main objective of the analysis was to evaluate how certain changes in some variables influence the energy production and, from these results, choose the geometric parameters of the RFL system, which will concentrate the greatest possible amount of energy

The first analysis to be made is about the effects of the quantity shift of reflecting mirrors in energy concentration in the receiver, as shown in Fig. 4.

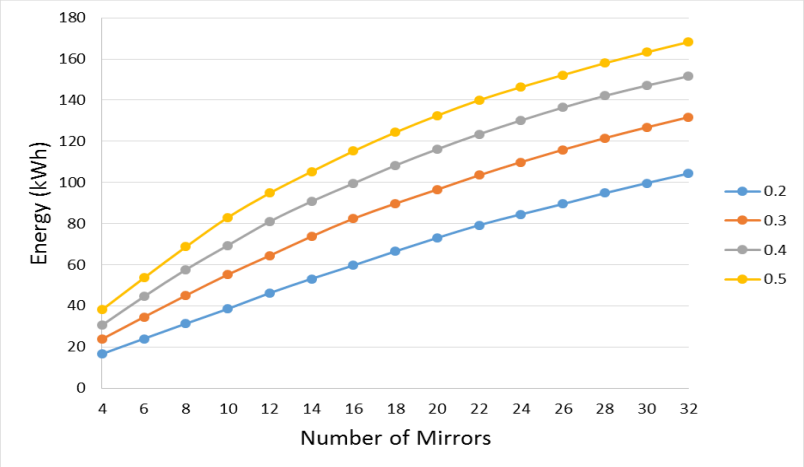


Figure 4. Received energy by the receiver as a function of the number of mirrors.

As can be seen in Fig. 4, the energy concentrated in the receiver increases in all cases of mirrors width. Also, with the increase of width and mirror number, the curve slope decreases more quickly. This indicates that the curves of larger widths reach a peak sooner than the curves of smaller widths. The reason this occurs is that as larger the mirrors become, more distant are the mirror arrays and greater are the losses.

The next analysis is to understand how the receiver height affects the energy concentration in the receiver. The graphic representation of this analysis can be seen in the Fig. 5.

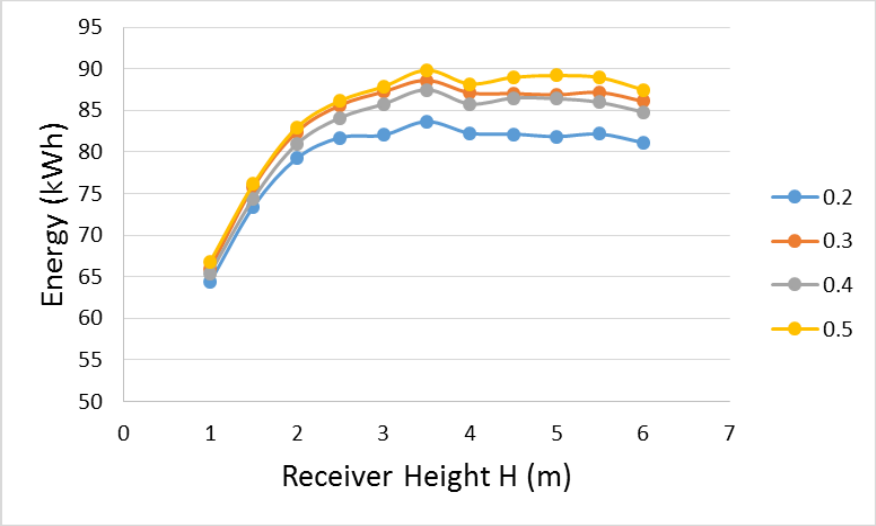


Figure 5. Received energy by the receiver as a function of receiver height.

From the graph above, it can be noted a rapid curve growth of all mirror widths up to a certain height. This is due to the reduction of blocking loss and shading by the receiver with the increase of receiver height. It also identified the height of 3.5 m receiver as the most efficient to energy concentration, considering the informed settings.

The following analysis is how the distance between the mirrors influences the efficiency of the heliostats system. The graphic representation of this analysis can be seen in the Fig. 6.

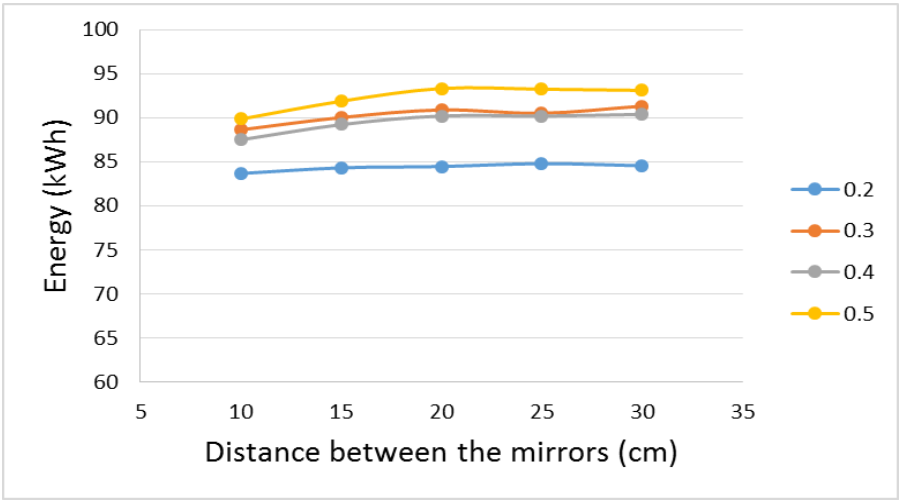


Figure 6. Concentrated Energy by the receiver as a function of the distance between mirrors.

According to the figure above, the inclination of the curves are very small and there is low increase in the energy concentration with the increase of the distance between mirrors. The reason this occurs is that with increasing distance between the mirrors, lower are the losses by blocking and shading. However, the distance between the receiver and mirrors becomes bigger, thereby increasing though the spillage loss, shading by receiver and cosine effect.

Thus, from the graphs generated in Figs. 4, 5 and 6, it is observed that the curves which showed higher amount of concentrated energy were from the mirrors with a width of 0.3 m und 0.5 m.Then, to know which configuration should be applied in the system, it was generated a graph with the efficiency that can be seen in Fig. 7.

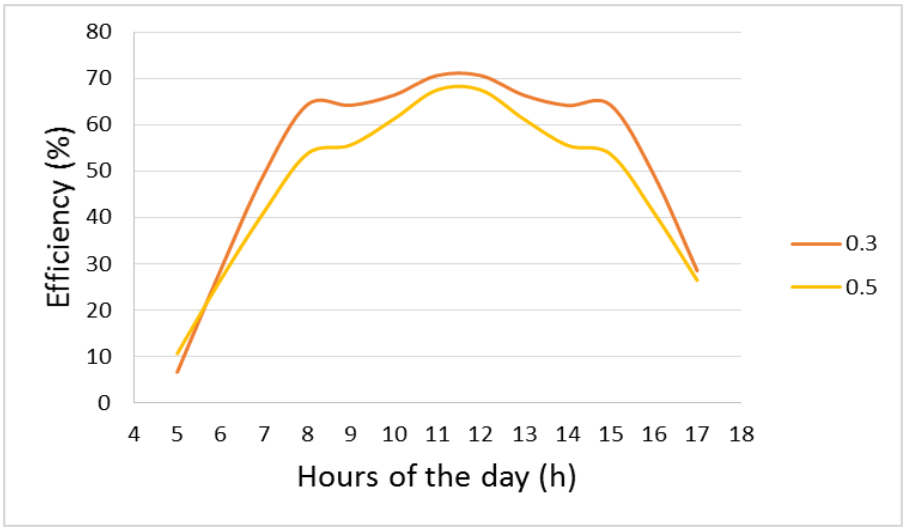


Figure 7. Efficiency of the mirrors during the day.

It is noticed that the configuration of mirrors with a width of 0.3 m, even producing less energy, is more efficient than that of mirrors with a width of 0.5 m.

After all the sensitivity analisys, the parameters from the energy concentration system were defined, as shown in Tab. 1.

Table 1. Defined variables from the System

| | |
|---|---|
| Number of Mirrors | 16 |
| Receptor Height | 3.5m |
| Receptor Width | 0.4m |
| Mirror Width | 0.3m |
| Distance between the mirror centers | 0.4m |
| Mirror Length | 3m |

Having the optimized parameters of the solar concentration system, it is possible to simulate daily energy concentration in the receiver in any city in the southern hemisphere of the planet. For this, it is necessary only the DNI data and the amount of Sun's hours from the place to be analyzed.

The concentration of daily energy that the city of Natal / RN, Brazil concentrates in the receiver were evaluated in this work. The data used for this simulation were achieved through CTGÁS-RN, which captured the DNI data from every hour of every day of the months of June 2015 to January 2016.

From these data, it was made the average DNI of every hour of every day of every month. It is noticed through these values that almost during all year, Natal / RN has 13 daily sun hours that are between 5 am and 18 pm. With this information and the information from the Tab.1, Fig. 8 was created.

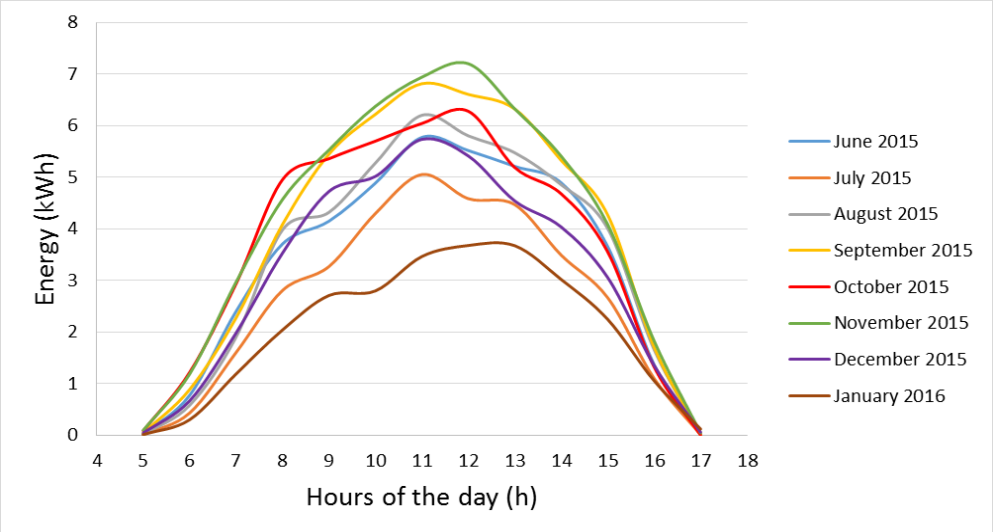


Figure 8. Average daily energy production in a few months in Natal with the optimized system parameters

Note that the months which have higher values of DNI, and consequently, greater concentration of power in the receiver are September, October and November. The months with the lowest concentration of energy shown in the fig. 8 are January and July and between them is that normally occur rainfalls and atmospheric attenuation, according to the UFRN Climatological Station.

## 4. CONCLUSIONS

In this work was shown the importance of sensitivity analysis to understand how some variables influence the loss mechanisms and efficiency of the energy concentration system. Moreover, this analysis was used to determine which parameters should be chosen to optimize the system from some initial design requirements. It can be concluded that the model that simulates the loss calculation and the efficiency of energy concentration system of a LFR plant for one day presents reasonable results and can be used in other locations. Moreover, from the graphs generated for Natal/RN, indices of energy concentration in the receiver show that the city has great potential for energy production from solar radiation. Another important fact to note is that the incidence of solar radiation in Natal/RN is high and keeps relatively constant throughout the year, as in other cities of the Northeast.

## 5. REFERENCES

Baharoon, D. A., Rahman, H. A., Omar, W. Z. W. and Fadhl, S. O., 2014. "Historical development of concentrating solar power technologies to generate cleane lectricity efficiently – A review". Renewable and Sustainable Energy Reviews, Vol. 41, pp. 996–1027.

Cordeiro, P., 1998. START Mission to Brazil. SolarPACES report No.2/98. Sandia National Laboratories, Albuquerque, NM, USA.

Duffie, J.A. and Beckman, W. A., 2013. Solar Engineering of Thermal Processes. John Wiley & Sons, Hoboken, NJ, USA.

Eustáquio, J.V.C.S., 2011. Master Degree thesis, Simulação e analise do comportamento do campo de heliostatos de uma central de concentração Solar termoeléctrica de receptor central. Faculdade de Engenharia da Universidade do Porto, Porto, Portugal.

Goswami, D. Y., 2015. Principles of Solar Engineering. Taylor & Francis Group, Boca Raton, FL, USA.

Mathur, S.S., Kandpal, T.C. and Negi B.S., 1991. "Optical design and concentration characteristics of linear Fresnel reflector solar concentrators – II Mirror elements of equal width". Energy Conversion and Management, Vol. 31, pp. 221-232.

Raia, M. F. R., 2016. BIG – ANEEL Setembro 2013. Matriz de Energia Elétrica Brasileira em 2013. Brazil, 12 Jun. 2016 <http://slideplayer.com.br/slide/337221/> .

Sattler, J.,O'Connell, B. And Norton, D., 2012. "Chapter 8 Solar Tower Technology". Advanced CSP Teaching Materials.

SolarGIS, 2014. Direct Normal Irradiation (DNI) Brazil. Brazil, 05 Jun. 2016 < http://solargis.com/assets/graphic/free-map/DNI/Solargis-Brazil-DNI-solar-resource-map-en.png>.

Tipler, P. A. and Mosca, G, 2012. Física para Cientistas e Engenheiros. Vol. 2. LTC, Rio de Janeiro, RJ, Brazil.

Walker, G.S., 2013. Development of a low cost linear Fresnel solar concentrator. Master of Science Thesis, Faculty of Engineering at Stellenbosch University.

## 6. RESPONSIBILITY NOTICE

The authors are the only responsible for the printed material included in this paper.